Results in Engineering 28 (2025) 108239

Contents lists available at ScienceDirect

Results in Engineering

journal homepage: www.sciencedirect.com/journal/results-in-engineering

Experimental study supported by ANN of new fabricated wall integrated with PCMs for energy saving and temperature uniformity of air-conditioned buildings

R.M. Saleh [a], Mahmoud Said [a,b,*], W.G. Alshaer [a], S.A. Nada [a,b]

[a] Mechanical Engineering Department, Benha Faculty of Engineering, Benha University, Benha, Egypt
[b] Egypt-Japan University of Science and Technology, Alexandria, Egypt

A R T I C L E I N F O

Keywords:
Prefabricated walls
Extruded polystyrene XPS
PCM cavity
Artificial Neural Network (ANN)
release time
Liquid fraction
Energy saving
walls configuration

A B S T R A C T

The building of walls comprises numerous layers to protect against external environmental variations. Increasing layers through the integration of PCM into the wall as a separate layer improves daily temperature regulation inside buildings but reduces floor area, resulting in no economic justification. This study establishes a design approach for PCM walls by creating two wall configurations. Then, experimental testing and predictive modeling were conducted using Artificial Neural Network (ANN) trained by Feed Forward Back Propagation (FFBP) algorithm to assess thermal performance under different environmental conditions and various locations within the prefabricated wall. The thermal behavior of the new fabricated walls is tested and evaluated using external surface temperature, internal surface temperature, and average daily heat fluxes, in contrast to a reference wall. The results show that the configuration (2) is the best configuration for reducing outer surface temperature by 3 °C and reducing inner surface temperature by 0.53 °C at various outdoor temperatures. The location of PCM in prefabricated wall near to the outside wall is the optimum location in the summer season rather than the inside wall. The average daily energy saving decreases gradually with increasing the ambient temperature. in configuration (2), the energy saving is about 20 % higher than in configuration (1) at different ambient temperatures. Also, the artificial neural network model demonstrates high accuracy in predicting temperature profiles and energy savings without including ambient temperature in the training data set. It turns out that the predictive model agrees with the experimental tests, with the minimum and maximum relative errors for indoor and outdoor temperatures being 0.5 to 2 % and 2 % to 4 %, respectively.

1. Introduction

The building and construction sectors account for approximately 36 % and 37 % of the total energy consumption and resulting CO2 emissions [1]. To reduce emissions of greenhouse gases, it is essential to use effective measures that regulate building energy usage and limit the growth of carbon emissions. The design of the building's envelope and choice of materials are closely connected to the building's energy consumption. In contrast to conventional heavy envelope structures such as reinforced concrete and blocks, lightweight envelope structures primarily use materials such as extruded polystyrene (XPS), expanded polystyrene (EPS), EPS foam mortar, polyurethane foam (PU), and various lightweight, porous inorganic insulation materials. While these materials offer effective thermal insulation, their reduced heat capacity may result in significant variations in interior temperature[2–5]. Therefore, it is essential to increase the thermal performance of the envelope, augment its thermal resistance, and minimize the need for heating and cooling loads. The application of phase change energy storage can improve inner thermal conditions and reduce building energy costs, resulting in increased use of PCMs in building envelopes. As a result, many experiments and theoretical studies have been conducted to determine how phase change materials affect the ability of walls to transfer heat. W. Li et al. [6] conducted an experimental and computational analysis to investigate the effects of phase change material (PCM) configuration, PCM thickness, and heat flux on the thermal efficiency of this lightweight envelope room. The findings demonstrate that the best temperature regulation was achieved with a 15 mm-thick phase change material on the interior side, resulting in a 2.4 °C decrease in the room temperature.M.A. Abdelkareem et al. [7] conducted a simulation study on four wall constructions to examine the influence of PCM on the thermal performance of lightweight construction walls in Sharjah, UAE.

* Corresponding author.

https://doi.org/10.1016/j.rineng.2025.108239
Received 5 October 2025; Received in revised form 2 November 2025; Accepted 14 November 2025
Available online 15 November 2025

Nomenclature

ANN	Artificial Neural Network
C_p	Specific heat of cement board, kJ/kg∘c
C_{xps}	Specific heat of Extruded polystyrene, kJ/kg∘c
C_{pcm}	Specific heat of PCM, kJ/kg∘c
Config.1	Configuration 1
Config.2	Configuration 2
ES	Energy saving
FFBP	Feed-forward back-propagation
GMDH	Grouped-Method of Data-Handling
ML	Machine learning
MSE	Mean squared error
NSGA III	Non-dominated Sorting Genetic Algorithm III
PCM	Phase Change Material
Q	Heat release, kJ
R	Regression value
Ref.	Reference wall
SVM	Support Vector Machine
T	Temperature, °C
t	Time, hr
T_m	Melting temperature of the PCM, °C
$T_{w,\ in}$	Inner wall temperature, °C
$T_{w,\ out}$	Outer wall temperature, °C
$T_{w,\ out,\ p}$	Outer surface temperature Infront of PCM, °C
$T_{w,\ out,\ xps}$	Outer surface temperature Infront of XPS, °C
$T_{w,\ in,\ p}$	Inner surface temperature Infront of PCM, °C
$T_{w,\ in,\ xps}$	Inner surface temperature Infront of XPS, °C
$T_{P,\ C1}$	Phase change temperature inside cavity 1, °C
$T_{P,\ C2}$	Phase change temperature inside cavity 2, °C
$T_{P,\ C3}$	Phase change temperature inside cavity 3, °C
$T_{P,\ C4}$	Phase change temperature inside cavity 4, °C
$T_{avg,\ P}$	Average phase change temperature, °C
T_R	Room temperature, °C
U	Uncertainty
x	Thickness, mm
XPS	Extruded polystyrene
δ	Liquid fraction
λ	Thermal conductivity, W/m∘c
ρ	Density, Kg/m^3
τ	Discharge time, hr

Subscript

Avg.	Average
C	Cavity
in	Inner
out	Outer
P	Phase change material
W	wall
xps	Extruded polystyrene

Outcomes indicated that the PCM significantly improved thermal stability, reduced fluctuations in inner wall temperature, maintained a temperature between 26 °C and 27 °C, and reduced heat flux by approximately 78.6 %. Moreover, the maximum energy conservation can be achieved by employing PCM in the roof and on south-facing surfaces. Z-a Li et al. [8] conducted experiments and simulation models to investigate the efficiency of phase change materials for temperature regulation in lightweight structures. The findings indicate that PCM can reduce peak temperature by 4.9–12 °C, raise the minimum temperature by 1.1–2.8 °C, and extend thermal comfort hours by 2–5 h. These structures can achieve reductions of 18.69 % and 49.63 % in peak cooling demands during summer transitional seasons, respectively. Furthermore, with an enhanced delay period of 2.67–4 h compared to the reference wall. Anter et al. [9] investigated the long-term thermal efficiency of a building wall in Aswan, Egypt, during the summer season, with and without integration of PCM. The results demonstrated that PCM application reduces wall temperature and indoor heat flux. RT-35HC had the superior thermal performance. Nair et al. [10] conducted an extensive analysis of household thermal heating applications employing phase change materials (PCM). They investigated novel approaches, essential factors, and the wide range of accessible PCMs.

Recently, several investigations have focused on the impact of the PCM layer's placement on the overall efficiency of the building [11–20]. Al-Absi et al. [16] indicated that the perfect placement of the PCM layer is significantly influenced by climatic conditions, intended application, PCM melting temperature, latent heat, the mass of PCM, thermophysical parameters of wall materials, mechanical cooling or heating, and wall orientation. The positioning of a PCM layer inside a wall is determined by the thermal characteristics of the PCM and outside conditions, as indicated by the studies of Jin et al. in References [17] and [18]. The researchers observed that when the melting point, heat of fusion, and thicknesses of the PCM rise, the best position of the PCM inside the wall begins to migrate towards the exterior surface. Conversely, as the temperature of the interior surface rises, the optimum position of the PCM shifts nearer to the interior surface. Refahi et al. [19] examined the installation of two PCM wallboard layers and an insulating layer in the outer walls of a four level building located in Tehran. The results indicated that using two layers of PCM with different melting temperatures can reduce the building's cooling and heating energy consumption in comparison to a single-layer configuration. Sun, X., et al. [20] developed a mathematical model to evaluate PCM performance in three test walls, aiming to find the best placement for heat fluxes with a reference wall. The results indicated that the fourth layer was most effective during winter, while the third layer was optimal for both summer and annual performance. Energy savings were 17.7 %, 20.2 %, and 23.1 % when PCM was placed in the first, second, and third layers, respectively.

A significant quantity of researchers advocates locating the PCM layer nearer to the source of heat.

Jahangir Khan et al. [21] performed an experiment to determine the optimal position of the PCM layer in a building wall structure. The results showed that placing the PCM layer closer to the source of heat, specifically on the inner wall surface instead of the outer surface, led to slight improvements in thermal efficiency and reductions in temperature fluctuations. Cao et al. [22] discovered that placing the PCM layer nearer to the outside environment enhanced efficacy. A numerical simulation assessed heat transfer efficiency in a residential building in Oslo, Norway, featuring multi-layer walls with advanced phase change materials. The study also indicated that increasing insulation thickness and reducing the thermal conductivity significantly reduces energy consumption in buildings.

Arici, M. et al.[23] investigated study of the thermal efficiency of external building walls containing phase change materials (PCM) for both cooling and heating loads. The results show that putting PCM between the insulation and external plaster saves the most energy during heating conditions. On the other hand, putting PCM between the internal plaster and concrete saves the most energy during cooling conditions.

The optimal positioning of the PCM layer is significantly influenced by its melting temperature. Lagou et al. [24] conducted a numerical analysis to determine the optimal positioning of PCM inside the building structures, focusing on suitable melting temperatures for PCM in six European cities across summer and winter. They recommend placing the PCM layer within the inner wall layer for all scenarios, with optimal

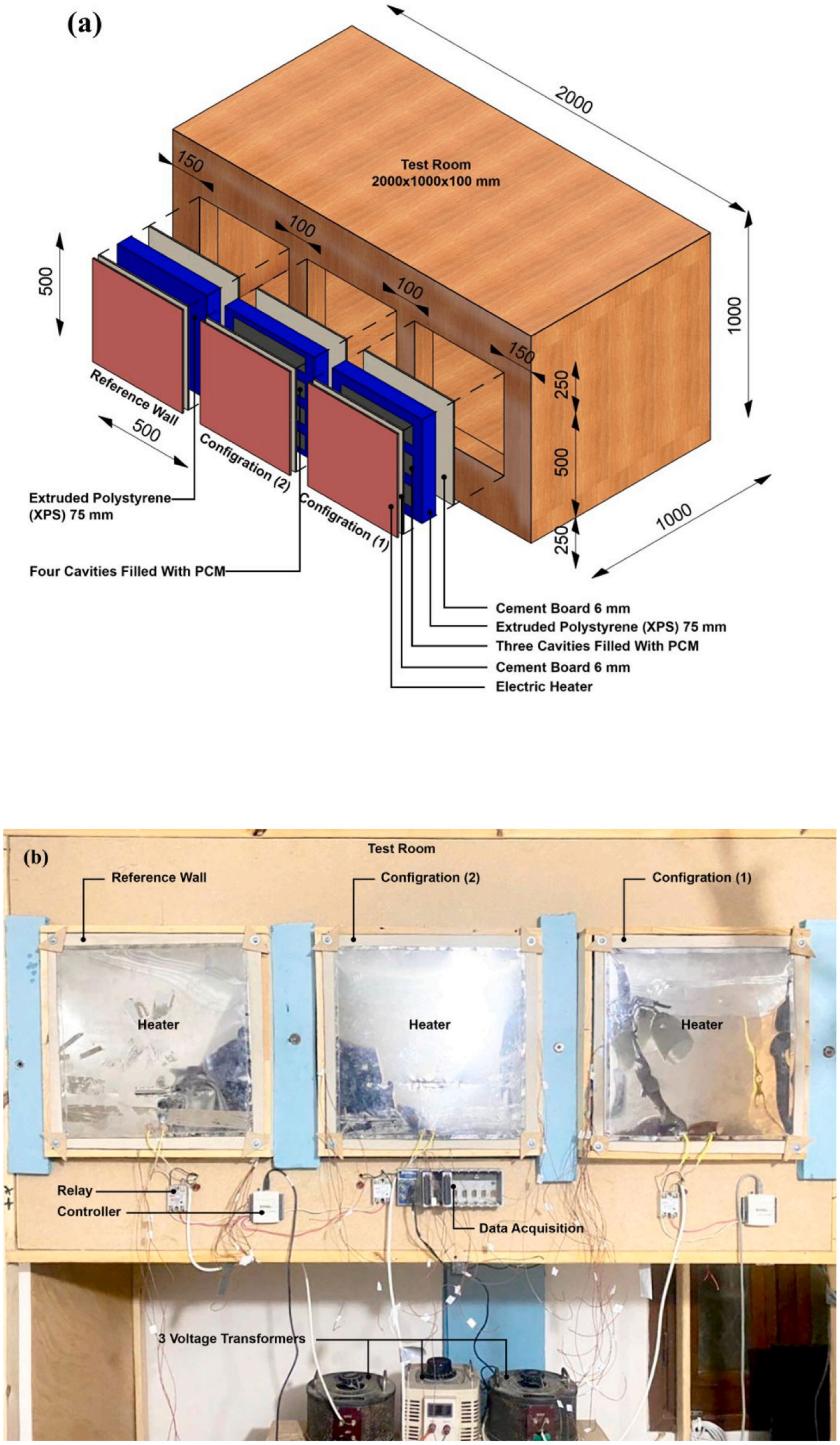

Fig. 1. (a) Illustration of the experimental setup in schematic form. (b) A photograph of the experimental set up.

melting points of 16 °C, 11 °C, and 20 °C for the southern, central, and northern regions, respectively, for optimal thermal performance. Darvishi et al. [25] conducted a numerical analysis to determine the optimal positions of three types of phase change materials with melting temperatures of 21, 23, and 25 °C. The analysis focused on two cities in Iran with divergent climatic conditions. The researchers concluded that integrating PCM in the middle region of indoor spaces, whether by direct placement or proximity, results in decreased thermal load and enhanced annual energy conservation, regardless of prevailing climate conditions. The performance of PCM combined LBW is greatly affected by various factors, including the PCM's position, latent heat, thickness, thermal conductivity, density, and phase transition temperature [26].

Data-driven strategies have become increasingly common for evaluating energy use in buildings [27]. Machine learning (ML) prediction

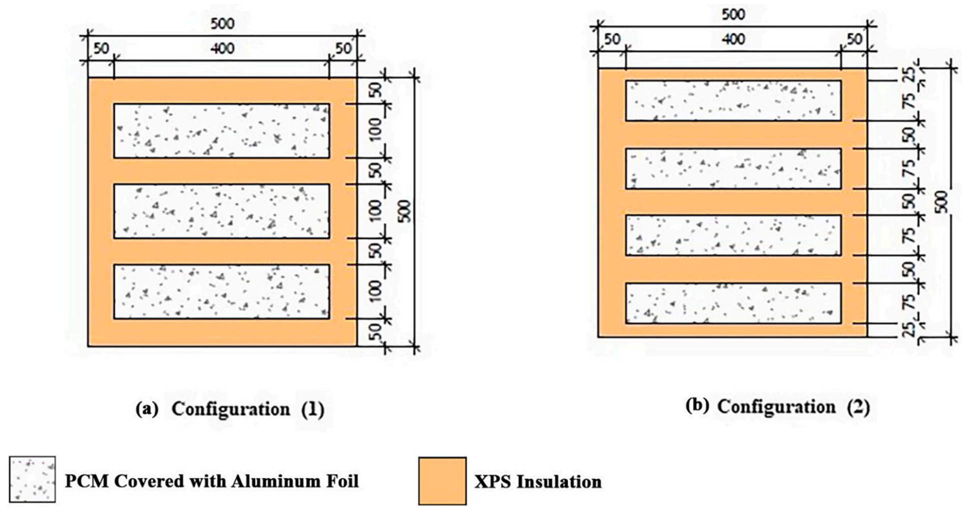

Fig. 2. Front view sections of the two tested walls showing PCM cavities locations and dimensions.

models can assess building energy consumption to support informed decisions in the construction of energy-efficient structures, using a database grounded in physical modelling. Machine learning approaches can reveal hidden layers of connections between independent and dependent variables in extensive datasets by employing statistical models as well as algorithms to produce forecasts for automating decisions that focused on establishing energy-efficient buildings with limited resources [28]. In this regard, various researchers [29–33] have provided the most effective forecasting models to estimate building performance without PCM, aligning with the established goals of their studies by applying multiple machine learning algorithms. Machine learning approaches utilize PCM integrated into buildings to evaluate energy consumption in building structures [34] . These methods can yield an optimal selection of the PCM layer's thickness, melting temperature, and kind of PCM for the design of energy-efficient buildings, utilizing simulated or experimental databases. An optimized, high-performing machine learning predictive model for assessing the performance of buildings using phase change materials, taking into account building envelope attributes, environmental factors, and energy efficiency strategies, may produce generalized outcomes based on fresh data. Constructing building situations and climates, thereby minimizing expensive experiments and numerical simulations [35–37]. Yang et al. [35] enhanced the efficiency of PCM-integrated buildings using the Non-dominated Sorting Genetic Algorithm III (NSGA III) and developed an energy consumption (EC) prediction model through a stacking machine learning approach in Shenzhen, China. The stacking model outperformed eight different ML models, showing a high correlation efficiency ($R^2 = 0.97$) in predicting energy consumption. Bagheri-Esfeh et al. [36] investigate the performance of cooling and heating when integrating PCM in residential buildings in Tehran by using the Grouped-Method of Data-Handling (GMDH). The results demonstrated that the R^2 value was above 0.9 for both heating and cooling energy, validating the accuracy of forecasting models. In another investigation, Zhussupbekov et al. [37] developed prediction models using ANN, SVM, and regression to estimate monthly energy consumption of PC-integrated systems based on a database related to architectural design elements. The ANN model was the most effective, achieving an R^2 value exceeding 95 % for predicting energy consumption in PCM-integrated buildings.

Most previous studies on this topic demonstrate that the performance of PCMs used in walls has been widely evaluated as a separate layer integrated into building construction for specific climatic conditions, proving their effectiveness in reducing energy consumption and enhancing indoor thermal comfort. Furthermore, recent research has used the Artificial Neural Network (ANN) to analyse the performance of PCM integrated into buildings, without focusing on the main aim of ANN: predicting temperatures and heat flux through the wall, and without including ambient temperature in the ANN training data set. Accordingly, the current research presents an experimental and modelling study on the thermal performance of a prefabricated wall enhanced by integrating PCMs. An experimental setup is established to test different configurations of PCMs-prefabricated integrated walls with different thickness and locations of the PCM layers inside the walls. Monitoring temperature profiles of the wall's layers and the PCM energy storage and release processes in summer for a wide range of climatic conditions is conducted. ANN modelling for predicting temperature profiles and heat flux throughout the wall is utilised. This step is accomplished to explore the possibility of applying ANN approaches in the design step of optimum PCM configuration. Thermal walls, heat gains, and building energy savings are investigated for the different wall configurations to determine the configuration with the best thermal performance.

2. Experimental setup

An experimental setup in the laboratory is designed and constructed to investigate and assess the performance of various prefabricated PCM-integrated wall configurations under different climate conditions. The main objective is to identify the optimal wall configuration that minimizes air conditioning power consumption in buildings and keeps the temperature level and uniformity conditions. The setup is equipped with the necessary instruments to regulate the test conditions like temperatures at different locations as well as to conduct accurate measurements of physical quantities required to analyze the system's performance. To figure out the best configuration for the prefabricated wall, the experimental setup is specifically developed to test the walls in both PCM charging and discharging modes.

2.1. Description of the experimental setup

The experimental setup comprises a temperature-controlled wooden test room with dimensions of 2 m in length, 1 m in width, and 1 m in height. The test room is located in a temperature-controlled laboratory via an air conditioning system. The long side wall of the room has three 500 mm x 500 mm openings/windows to be fitted with the tested walls, which have the same dimensions as the windows and a 87 mm thickness, as shown in Fig. 1–a and Fig. 1–b. Each tested wall is covered on the outside with a heating plate connected to a variable-voltage transformer

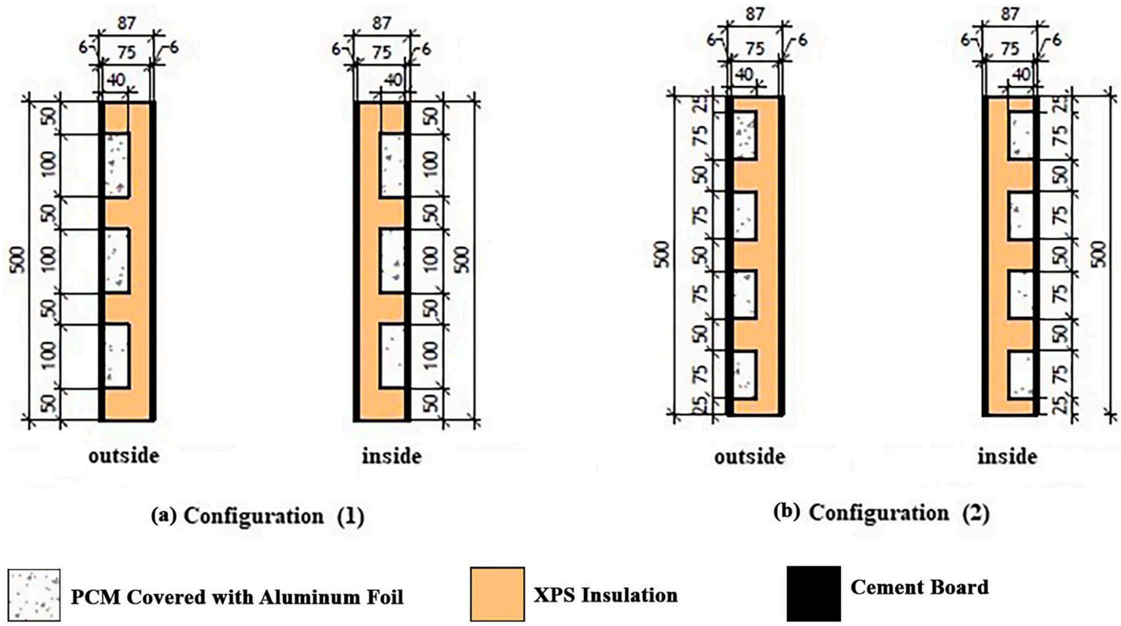

Fig. 3. Side section in the tested walls showing detailed dimensions and PCM location.

Table 1
Thermal Properties of wall materials.

Material	Density(ρ) (Kg/m^3)	Thermal Conductivity (K) (W/m°c)	Specific heat (C_P) (kj/kg°c)	Thickness (X) (mm)
Cement board	1100	0.164	840	6
XPS insulation	35	0.034	1500	75
Heating Plate	-	-	-	1

Table 2
Thermo-Physical properties of RT 24 (RUBITHERM® Data Sheet) [38].

Physical quantity	Value
Melting area	21–25 °C (Main peak 24 °C)
Congealing area	25–21 °C (Main peak 22 °C)
Heat storage capacity (±7.5 %)	160 kJ/kg
Specific heat capacity	2 kJ/kg.K
Combination of sensible and latent heat (in 15–30 °C range)	42 Wh/kg
Density solid (at 15 °C)	0.88 kg/l
Density liquid (at 35 °C)	0.77 kg/l
Volume expansion	12.5 %
Thermal conductivity	0.2 W/m.K
Maximum operation temperature	55 °C

to control its temperature. The three tested walls are named as the reference wall, configuration 1 and configuration 2. The construction of the three tested walls is shown in Fig. 1a. The reference wall consists of three layers: an internal and an external cement board layer of thickness 6 mm, and an extruded polystyrene (XPS) insulation layer of thickness 75 mm as the middle layer. In wall configuration 1, the XPS sheet has three rectangular cavities filled with PCM either in the inner or outer sides of the wall. Fig. 2-a. and 3-a. shows the geometric dimensions and locations of the three PCM cavities of configuration 1. The wall configuration 2 is like configuration 1, but it has four PCM cavities instead of three, with dimensions and locations as shown in Fig. 2–b and Fig. 3–b. The PCM cavities are filled with phase change materials of RT 24 type [38]. As per the manufacturer's data sheet, RT 24 has a phase change heat capacity of 160 kJ/kg for the transition from solid to liquid. The melting temperature of the RT 24 is within the range of 21–25 °C, which is close to the conditions typically considered comfortable indoors. RT 24 exhibits minimal volume expansion during the phase shift process, with an expansion rate of <12.5 %. The wall materials' properties are listed in Table 1, while the thermophysical specifications of the PCM material according to the manufacturer's data sheet are listed in Table 2,

The main thermo-physical properties of RT24 are measured and compared with the manufacturer's data sheet using the differential scanning calorimetry (DSC) procedure, and the results are found to be identical to the manufacturer's data sheet by Nazari Sam, M., et al. [39].

To simulate the walls during day and night, the wall heaters were on and off and the PCM go to charging (melting) and discharging (solidifications) conditions, respectively. To simulate the daytime in summer, the heater plate on the outer surface of the wall is turned on to heat the outer surface of the wall, and its temperature is regulated with the transformer until reaching the required value, which simulates the outdoor temperature. The heating power is intended to transfer by conduction through the wall thickness from outside to inside. In walls configurations 1 or 2, the phase change material (PCM) absorbs this heat, and subsequently, this heat does not reach the inner surface of the wall, causing a reduction of the room cooling load and maintaining the indoor temperature. During this process, the PCM undergoes a phase transition from solid to liquid charging phase. At night, the heaters were placed on off condition and the PCM start to solidify through the discharging process. The tests and processes were repeated at different conditions according to the following experimental program: wall outer surface temperature (Simulate day outdoor temperature) 35, 40 and 45 °C wall outer surface temperature (Simulate night outdoor temperature) 16–20 °C

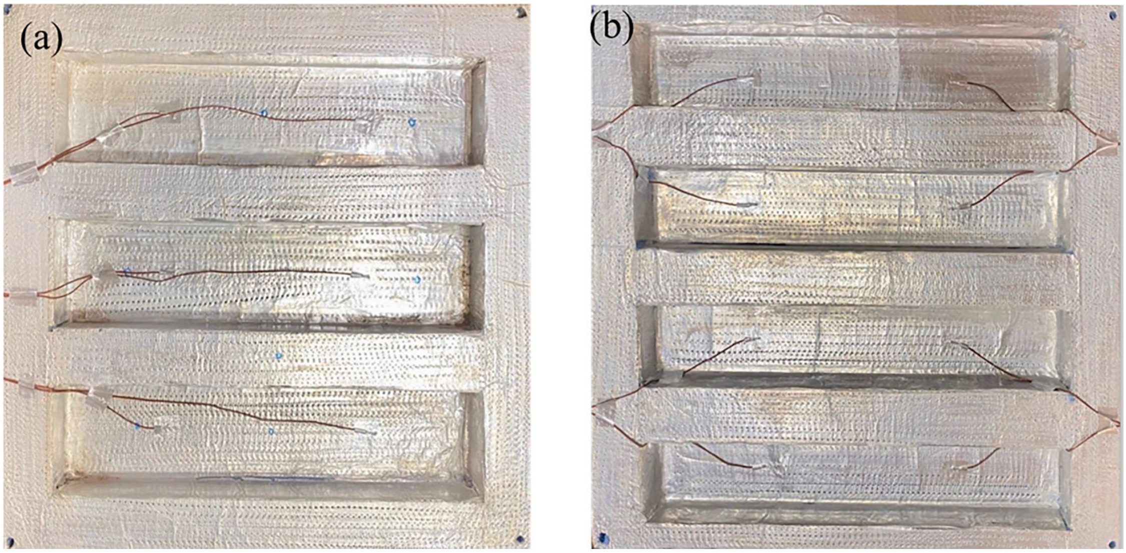

Fig. 4. Thermocouple distribution inside the Cavity (a) Configuration (1). (b) Configuration (2).

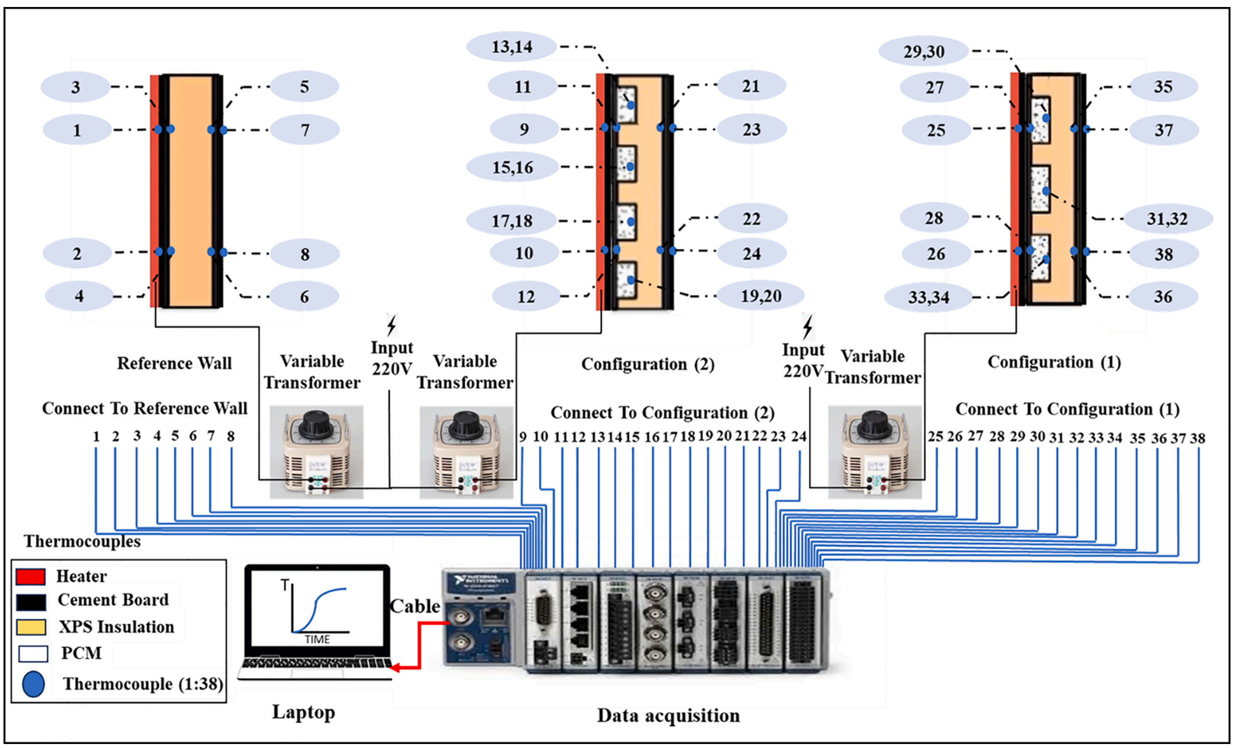

Fig. 5. illustrates the distribution of thermocouples in the various walls.

2.2. Instrumentations and measuring parameters

Temperature sensors are installed at various locations to measure the temperature. T-type thermocouples (copper/constantan) are used to measure the walls and PCM temperatures through the melting process. Two thermocouples are mounted on the outer layer (Cement Board) beneath the heating plate to measure the wall surface temperature. Two additional thermocouples are mounted on the inner surface of the outer layer (Cement Board) to measure the temperature distribution. Four thermocouples measure the inner and outer temperatures of the Cement board's inner layer. Each PCM cavity is equipped with two thermocouples to measure the transient temperature history during charging and discharging, as shown in Fig. 4. Fig. 5 illustrates the distribution of thermocouples in the various walls. Another thermocouple is used to measure the temperature in the test room. The thermocouple readings are calibrated using a standard thermometer of ±0.25 ºC accuracy. All the thermocouple wires are connected to a data acquisition system (National Instrument NI CDAQ- 9178). The thermocouples channel (National Instruments NI-9213) is inserted into the data acquisition and connected to the thermocouples wire to acquire and record their transient readings via a laptop. The data acquisition was adjusted and programmed to measure and record all temperature readings every 10 s. The data were extracted and recorded in an Excel sheet using the LabVIEW program. The uncertainty of the measurement parameters in the experiment was conveyed using the strategy by Moffat [40] according to the sensitivity of the measurement instruments and the minimum value

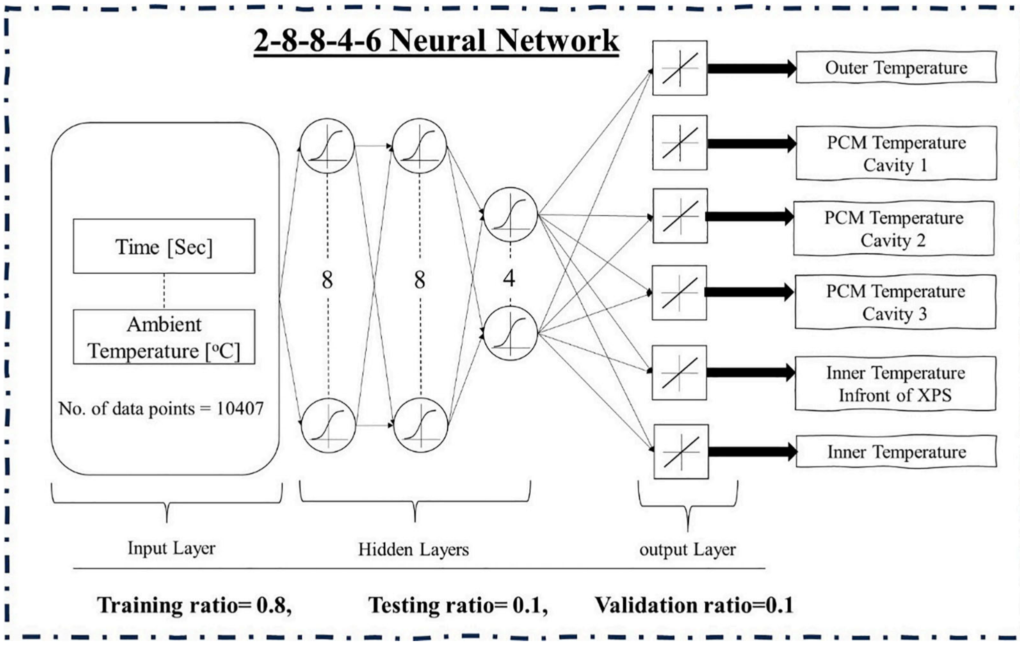

Fig. 6. Structure of ANN used in this study.

of each independent variable considered (by equation (1)).

$$U_x = \sqrt{\left(\frac{\Delta x_1}{x_1}\right)^2 + \left(\frac{\Delta x_2}{x_2}\right)^2 + \ldots + \left(\frac{\Delta x_n}{x_n}\right)^2} * 100 \tag{1}$$

The uncertainty in experimental can be refer to the inaccuracy of thermocouple and voltameter and ammeter has been estimated ±0.2ºC,0.3 % and 0.2 % respectively. Based on equation (1) the overall uncertainty in the experimental data was estimated and found in the range ± 2.5 %.

3. Artificial neural network (ANN) approach

An ANN is the preeminent computer approach employed to study and comprehend complex engineering challenges. This is a widely recognized and validated method for forecasting weather and experimental data. Of all methods ANNs have emerged as the most prevalent, capable of predicting complex results and reducing experimental time. The structure of the current study is illustrated in Fig. 6, comprising 2 input parameters and 6 outputs. The first input is the outer ambient temperature (i.e. heater set point 35 °C, and 45 °C), and the second input is the time at which the PCM temperature is measured. The outputs which represents thePCM temperature are outer temperature, temperature of PCM for Cavity 1, temperature of PCM for Cavity 2, temperature of PCM for Cavity 3 inner temperature in front of XPS, inner temperature. Moreover, the network includes 3 hidden layers with 8–8–4 neurons respectively. Prior to training the network, the data was standardized and divided into three sets: 80 % allocated for training the network, 10 % designated for testing the network, and 10 % validating its performance. The neural network was trained using conjugate gradient backpropagation with Polak-Ribiére updates algorithm 'traincgp'. The weights of the neurons are adjusted in the back propagation step to achieve the lowest error between the true and predicted value. Also, this training algorithm fits well with large size data set used in the training process. The current study employs two function activation for the brain's neural network. The "Tansig" activation function is employed across the input and hidden layers, whereas the "purelin" activation function is utilized thereafter. The function is utilized for the output layer. The quantity of neurons in a hidden layer is determined by a trial-and-error methodology.

4. Results and discussion

4.1. Temperature distribution for configuration (1) during charging process

Fig. 7 demonstrates transient temperature distributions of the inner and outer surfaces of the prefabricated walls and through the different sections of the wall's layers for the reference wall and configuration 1 wall. Also, the hourly transient temperatures inside the test room are shown in the Figure. The profiles are given for three simulated ambient temperatures, namely 35, 40 and 45 °C in Fig. 7-a, Fig. 7–b and Fig. 7–c, respectively. At the beginning of the simulation, it can be observed that the inner wall surface temperature in configuration (1) is less than that of reference wall, and the difference decreases gradually with time until it finishes, then the temperature of configuration 1 becomes higher than the temperature of the reference wall. This can be attributed to the fact that most of the heat that tends to transfer through the wall of configuration 1 is absorbed by the PCM to start the melting process and not reach the inner surface of the wall, and this absorbed heat decreases with time until complete melting of the PCM, causing the increase of the inner wall of configuration 1. However, in the reference wall, all the heat flux is transferred directly by conduction through the wall, rapidly raising the wall's inner surface temperature to its steady state value. After complete melting of the PCM, the inner surface temperature of Configuration (1) increases more rapidly than the inner surface temperature of the reference wall, as all the heat is transferred by conduction (no further part consumed in PCM melting), and due to the thermal conductivity of PCM being higher than that of XPS. So, it can be concluded that using PCM material in prefabricated walls contributes to reducing the inner surface temperature of the wall by 3 °C than reference wall. Also Fig. 7, shows that at the start, the interface inner temperature between the cement board layers and the XPS layer in configuration 1 is less that of the reference wall due to the heat absorbed by the PCM but the differences decreased with increasing the absorbed energy until it become lower than the reference wall temperatures after complete melting due to the high thermal conductivity of the PCM compared to XPS. The PCM liquefied and released the stored heat when the ambient temperature exceeded its melting point. Fig. 7 also indicates that the temperature of the phase change material (PCM) at the beginning of the experiment is nearly equivalent to its solidification

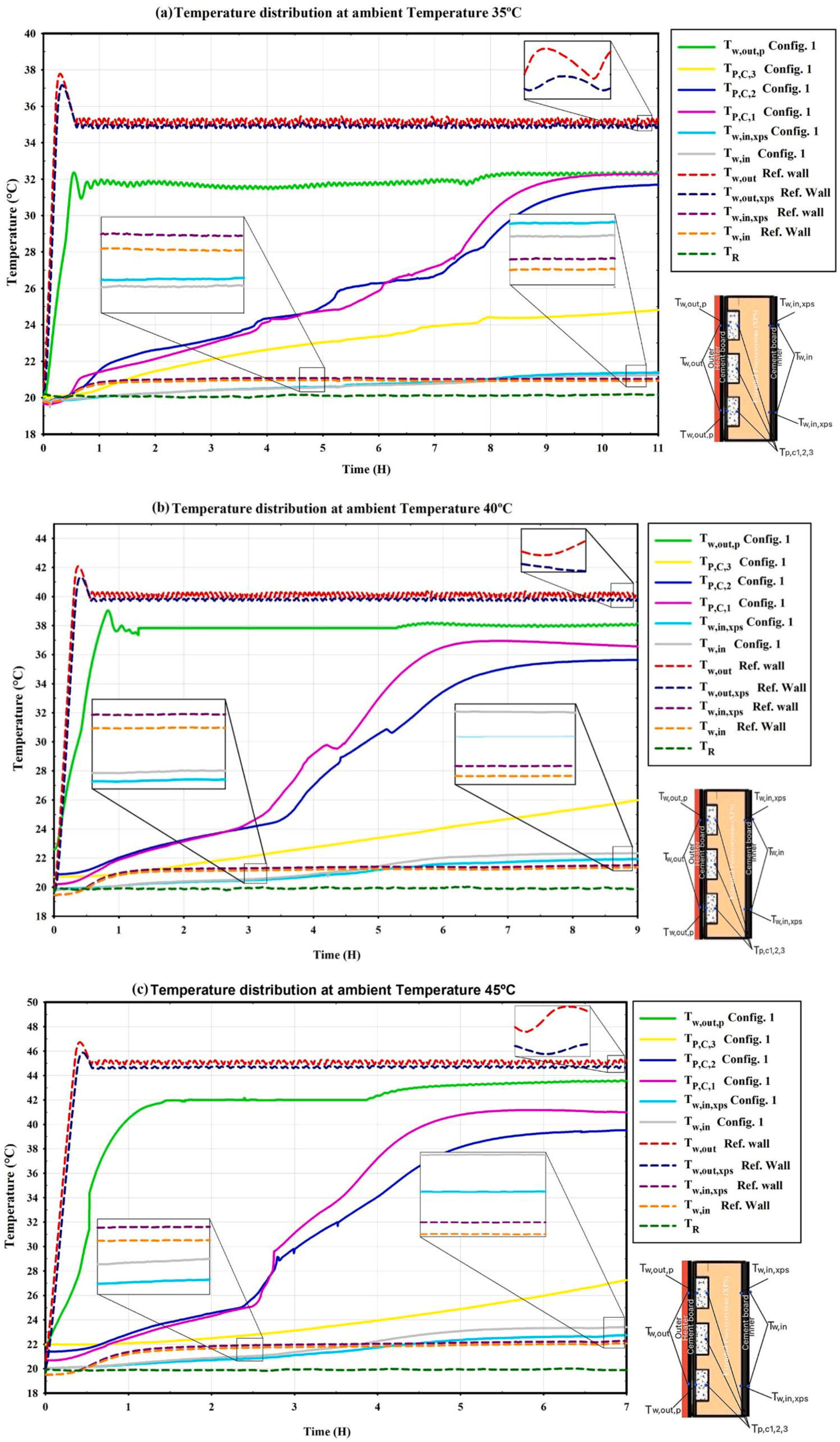

Fig. 7. Temperature distribution for Configuration (1) at different ambient temperatures.

temperature. As the discharge process begins, the temperature of the PCM increases gradually over time until the charging process is fully complete. The duration needed for the PCM to approach the outside temperature is referred to as the discharge time. The temperature of the PCMs at the upper position was dramatically higher than that at the lower position as the melting process occurred more rapidly for the PCMs positioned at the top. Nevertheless, the temperatures of the phase change materials (PCMs) at the upper and lower places converged

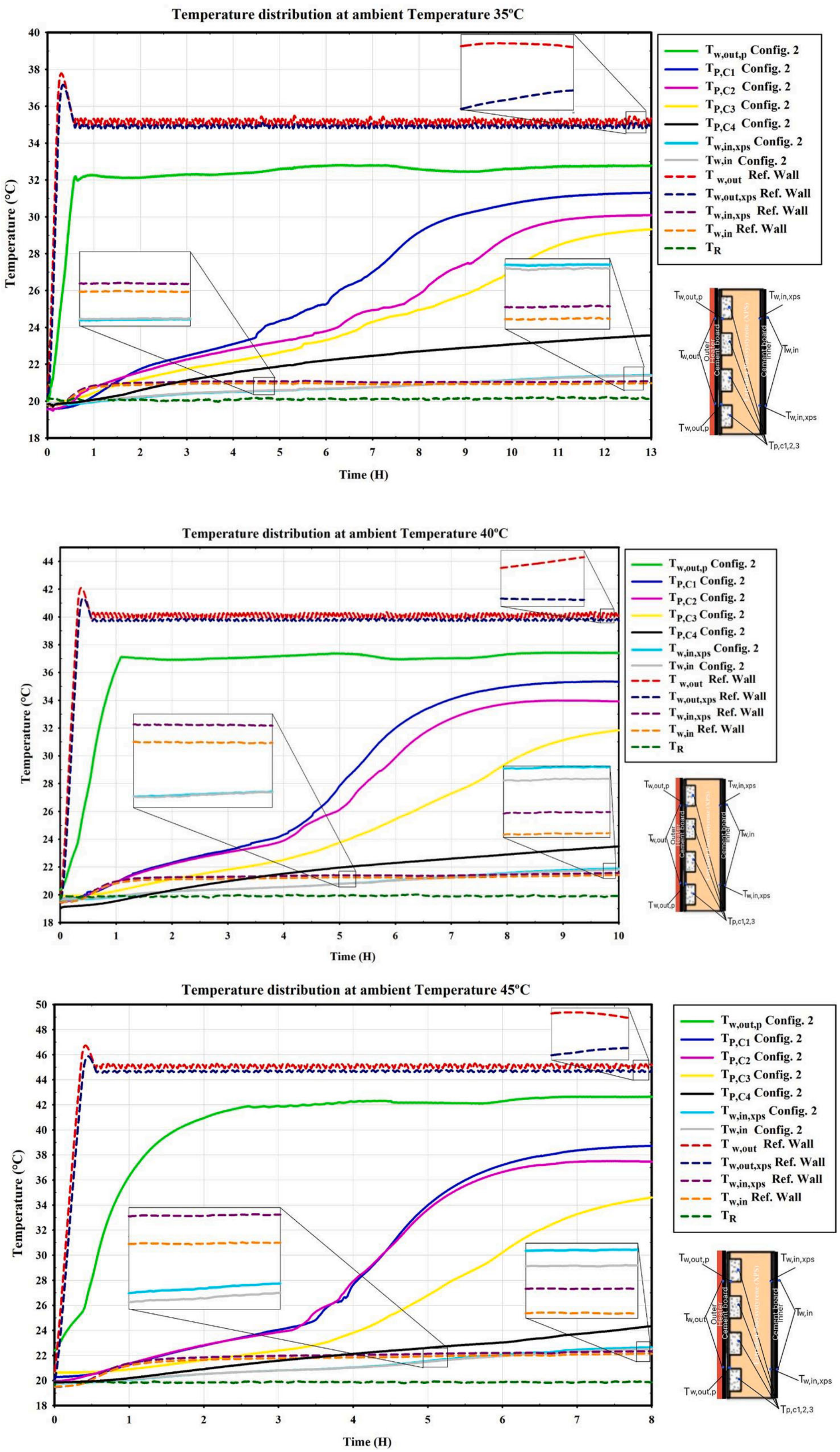

Fig. 8. Temperature distribution for Configuration (2) compared with the reference wall at different ambient temperatures.

during the solidification process. Additionally, Fig. 7 indicates that the external surface temperature between the cement board and the PCM cavities was lower than that of the reference wall. This is a result of the PCMs absorbing and storing the solar heat, comparing Figs. 7-a, b, and c reveal the reduction in discharge time in the PCM cavity when the ambient temperature rises from 35 40 to 45 °C. This is also ascribed to the augmentation of the heat transfer rate from the surroundings to the PCM cavity, resulting from an increased temperature differential, which

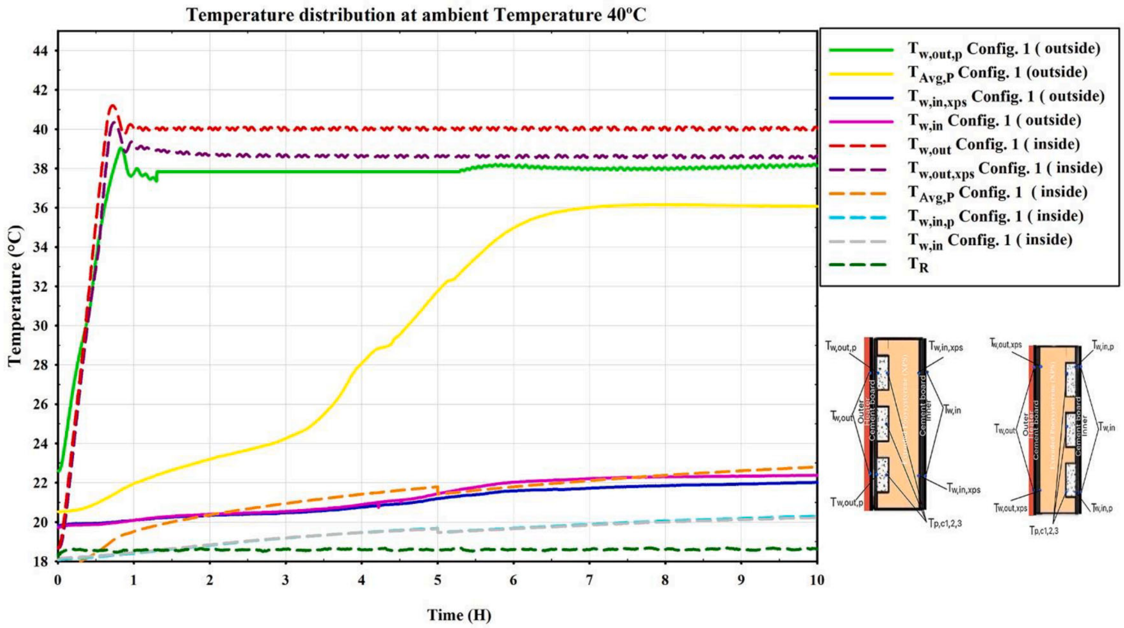

Fig. 9. Effect of PCMs layer location in the wall.

allows a more rapid discharge rate and a reduced discharge time. Also, the comparison shows that the external surface temperature between the cement board and the PCMs cavities is decreasing when the ambient temperature increases.

Fig. 8 illustrates the hourly transient temperature profiles for the wall configuration (2) compared with the profiles of the reference wall under various outdoor ambient temperature conditions that were adjusted using plate heaters, which simulate the solar heat flux. At the start and during the PCM melting inside configuration 2, the reference wall exhibited the highest exterior temperature compared with wall configuration 2. Also, the external cement board wall layer of configuration (2) has a lower temperature than the reference wall. This is because in configuration 2, the solar energy simulated by the heating plate was absorbed and retained within phase change materials (PCMs). The maximum temperature difference between the external surface temperature of configuration (2) and the reference wall at ambient temperatures of 35 °C, 40 °C, and 45 °C was approximately 3.1 °C, 2.7 °C, and 2.3 °C, respectively. Initially, during the melting process, the internal surface temperature of configuration (2) is lower than that of the reference wall at ambient temperatures of 35 °C, 40 °C, and 45 °C by 0.53 °C, 0.4 °C, and 0.25 °C, respectively. Throughout the entirety of the melting process, the internal surface temperature of the configuration (2) wall remained lower than that of the reference wall and after complete melting, the internal surface temperature of the reference wall became lower than that of configuration (2). Fig. 8 indicates that the discharge time decreased as the ambient temperature increased; it was 13 h, 10 h, and 8 h at ambient temperatures of 35 °C, 40 °C, and 45 °C.

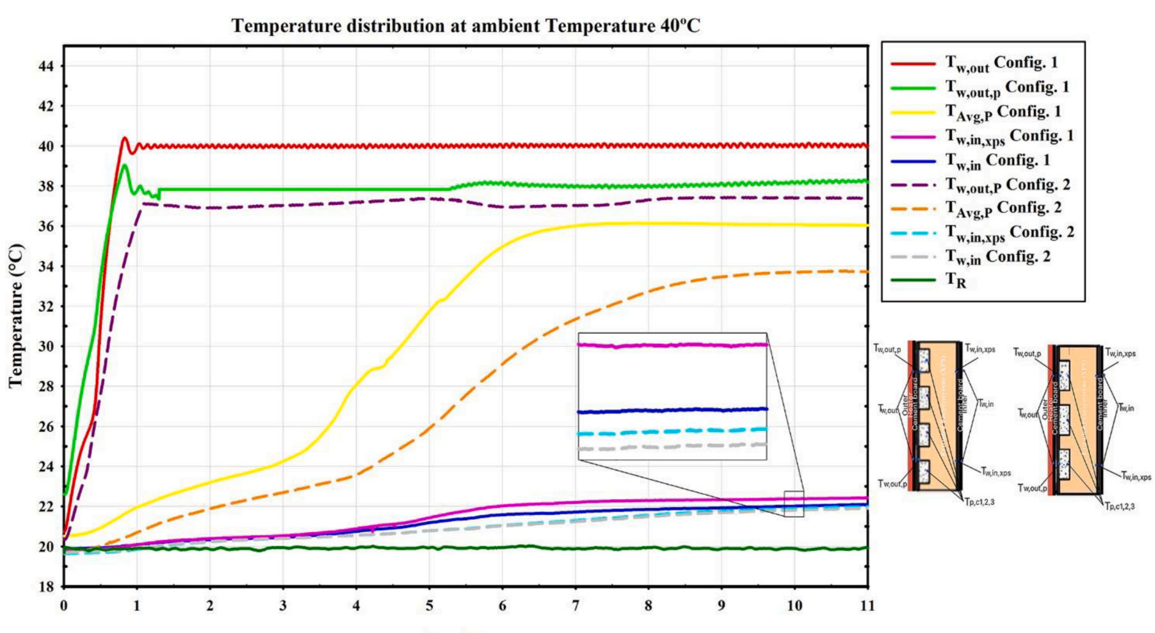

Fig. 10. Comparison between configuration (1) and configuration (2) at 40 °C ambient temperature.

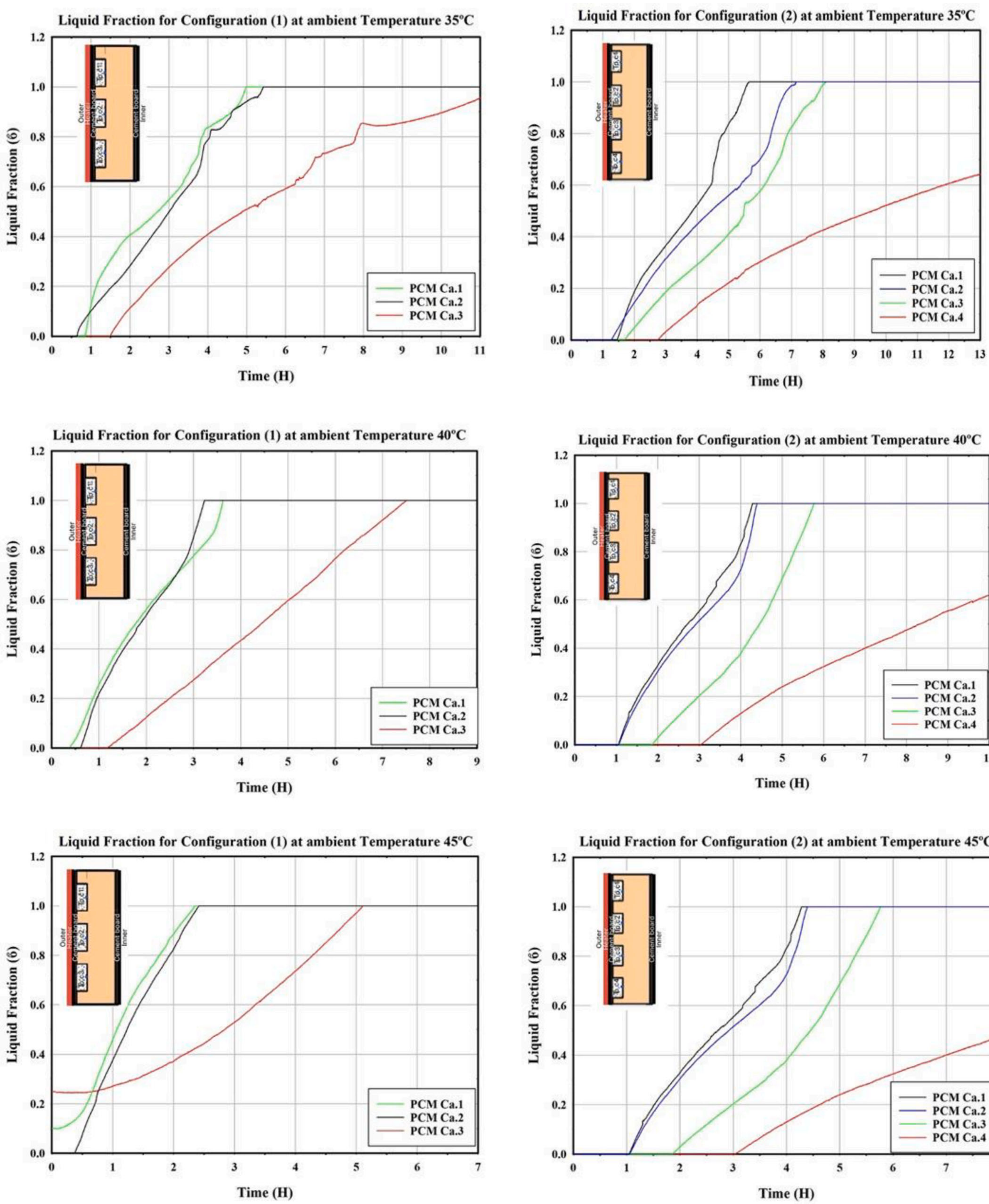

Fig. 11. Liquid Fraction for Configuration (1) and Configuration (2) at various ambient temperatures.

4.2. Effect of PCM location

Two placements of the PCM locations, near the outside or the inside cement wall layer, as shown in Fig. 3, were investigated. These two locations were named as near outside and near inside in the following discussion. The placement of the PCM within the wall dictates the degree of its interactions with the external surroundings and the indoor room. Fig. 9 illustrates and compares the temperature profiles performance of the wall of configuration (1) with both locations of the PCMs outside and inside locations. Fig. 9 demonstrates that placing the PCM near the outside wall surface lowers the peak temperature more than placing it near the inside location. Also, in locating the PCM near the outside, the PCM melting process/discharge occurred more rapidly and was completed faster, as it is very close to the outside surroundings. In addition, this location makes the transfer of the PCMs stored heat to the indoor room very slow and ineffective due to the substantial thermal resistance of the XPS wall layer. Similarly, when PCM has been placed adjacent to the inner wall surface, the melting process is not expected to be complete, and the internal surface temperature is lower than the internal surface temperature when PCM is located near the outside surface. However, it is suggested to place the PCM layer adjacent to the interior environment in building heating to use the accumulated thermal energy for regulating indoor air temperature during cold seasons. The same trends of the temperature profiles of the two locations of the PCMs in wall configuration 2 were noticed to be similar to those of configuration. So, it can be concluded that (i) in hot regions where air conditioning cooling is required, it is recommended to place the PCMs near outside and (ii) in cold regions where heating air conditioning is required, it is recommended to place the PCMs near the room indoor.

4.3. Comparison between configuration (1) and configuration (2)

Fig. 10 illustrates and compares the hourly temperature profiles of configuration (1) and configuration (2) at an ambient temperature of 40 °C as an example. It was clear that the peak temperature of the external wall for configuration (2) is slightly lower than the peak temperature for configuration (1) by 0.8575 °C due to the heat absorbed and stored from the PCMs in configuration (2) being higher than that in configuration (1). Furthermore, the average melting duration of the PCM in configuration (2) is 3 h longer than in configuration (1), likely attributable to the augmented thickness of the PCM, which results in an extended discharge time. Additionally, the internal surface temperature of configuration (2) is 0.4 °C lower than that of configuration (1), due to heightened thermal resistance and reduced heat transmission to the internal surface. The analysis clearly indicates that configuration (2) is the most efficacious approach for reducing indoor fluctuation in temperature So it can be concluded that augmenting the thickness of phase change materials (PCMs) improves the thermal resistance and mass of the wall, resulting in an extended discharge period.

4.4. PCM Liquid fraction profiles

Fig. 11 depicts the liquid fractions for configurations (1) and (2) at different ambient temperatures when phase change materials (PCMs) were positioned toward the outer surface of the wall. The phase transition of solidification and melting transpires at variable outside temperatures. Liquid fraction is a non-isothermal process, meaning it does not occur at a single temperature but over a Temperature range. When melting begins, once the local temperature exceeds the onset melting point, it continues progressively as heat penetrates deeper into the material. The shape and slope of the liquid fraction curves also reflect the heat transfer mechanisms and temperature gradients within the cavity. Positions closer to the heated wall reach higher temperatures earlier, resulting in a faster rise in liquid fraction and an earlier completion of melting. Conversely, regions farther from the heat source exhibit delayed melting due to weaker heat conduction and convective effects in the liquid phase. Consequently, the total melting time depends strongly on both the position and thermal boundary conditions. For simplicity, the calculation to estimate the liquid fraction assumed as a linear relationship between liquid fraction and temperature and ignores the complex, nonlinear behavior (the mushy zone dynamics), it introduces a variable known as the liquid fraction (δ), which may be computed using the Eq. (2) [41].

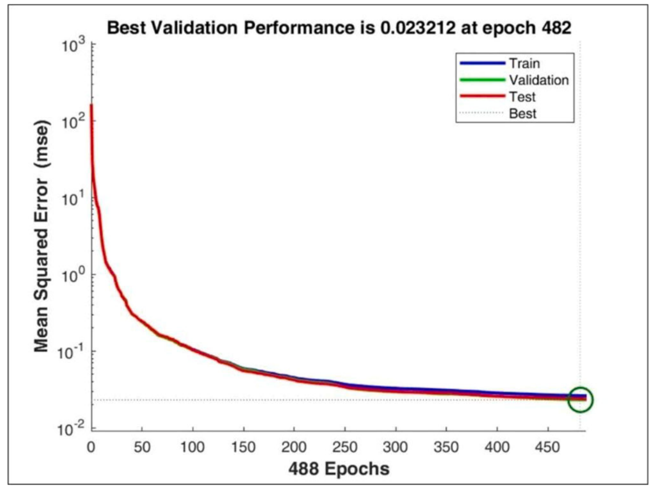

Fig. 12. Training, validation and testing losses of (ANN) model during training process.

$$\delta = \begin{cases} 0, & T < T_S \\ \dfrac{T - T_S}{T_L - T_S}, & T_S \le T \le T_L \\ 1, & T > T_L \end{cases} \tag{2}$$

Where T is Temperature and subscripts S,L represent the PCM solid and liquid temperature, respectively.in this study, the solidification temperature and liquid temperature of PCM are to $T_S = 21^{\circ}C$ and $T_L = 25^{\circ}C$.

Fig. 11 also shows that increasing the ambient temperature mainly reduces the PCM melting time across all configurations. The heat transfer behavior within the PCM cavity can be described by four distinct stages corresponding to the solid–liquid phase transition process [42]. In the initial stage, heat is conducted from the left wall into the PCM cavity, where conduction is the primary mode of heat transfer. As the PCM starts to melt, buoyancy effects intensify, leading to the gradual development of natural convection. Consequently, heat transfer occurs through a combined mechanism of conduction and convection. During the third stage, natural convection becomes the dominant heat-transfer mechanism. Once the melting is fully completed, the PCM's latent heat is depleted, marking the fourth stage in which heat storage takes place mainly in the form of sensible heat. Configuration (2) has a longer melting time than configuration (1) due to the greater number of cavities in the prefabricated wall. The melting time for configurations (1) and (2) decreases by 30 % and 40 % by increasing the ambient temperature from 35 °C to 40 °C and 45 °C. Therefore, increasing the number of cavities in the wall increases the melting time. This is because the decrease in cavity height near the outer wall reduces convection heat transfer inside the cavity.

4.5. Analyzing the performance of walls by (ANN)

The computational model has been trained from the gathered dataset at two ambient temperatures (35 °C and 45 °C) by utilizing output data such as outer, inner, and PCM melting temperatures from experimental testing. The training process was accomplished using the Polak-Ribiere conjugate algorithm. Fig. 12 displays the loss vs. epoch graph, which illustrates fluctuations in loss over the computational model's training process. The term "loss" denotes the error or deviation between the model's predicted output and the actual ground truth. The x-axis of the graph denotes the epochs, which are iterations across the complete dataset during training. Throughout training epochs, the model persistently updates and computes the loss, depicted on the *y*-axis of the graph. The model underwent 488 epochs to reach a minimum (MSE). A

Table 3
Evaluation of metrics for regression analysis [42].

Abbreviation	Parameters	Formula	Definition	Equation
R	Correlation coefficient	$R = \frac{\sum_{i=1}^{N}(y_i - y_i^{mean}).(\hat{y}_i - \hat{y}_i^{mean})}{\sqrt{\sum_{i=1}^{N}(y_i - y_i^{mean})^2].[\sum_{i=1}^{N}(\hat{y}_i - \hat{y}_i^{mean})^2]}}$	Indicates the strength and direction of the linear correlation between the actual and predicted values.	(3)
MSE	Mean Squared Error	$MSE = \frac{1}{N}\sum_{i=1}^{N}(y_i - \hat{y}_i)^2$	the average of the squared deviations between the actual and predicted values	(4)

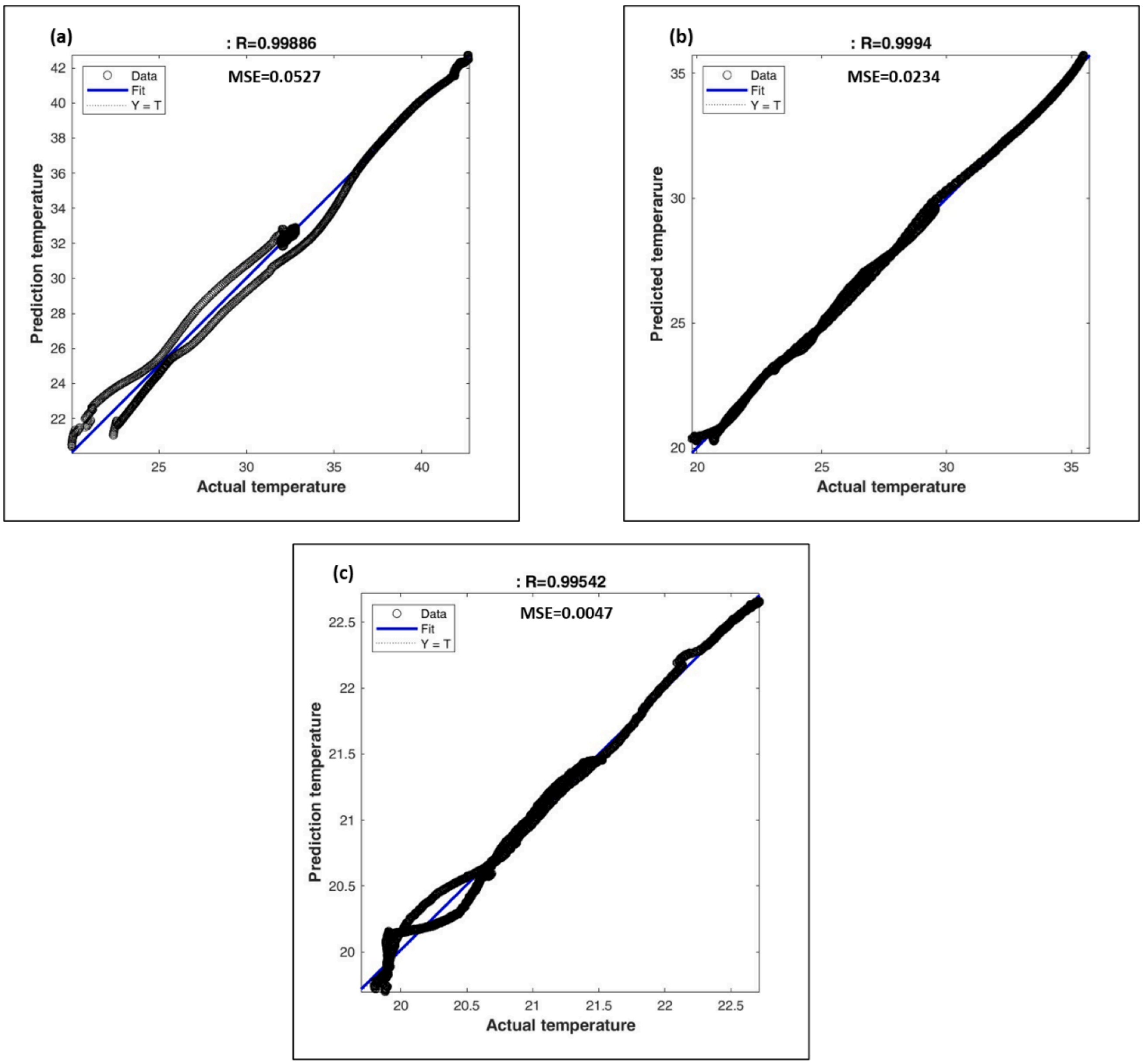

Fig. 13. Regression analysis of Training, validation, Testing through the wall (a) outer Temperature. (b) PCM melting temperature. (c) inner temperature.

declining loss trend signifies enhanced predictive ability, demonstrating the model's approach to optimal parameters. The assessment of training, validation, and testing datasets results in a final loss value of 0.023212 at epoch 482. These findings suggest that the FFB ANN is effective in predicting the outer, inner , and PCM melting temperatures of Configuration (2). The constructed ANN exhibits superior efficacy in predicting temperature versus time curves under various ambient temperatures, eliminating the need for a more intricate ML model. The machine learning performance metric is used to evaluate model accuracy. The regression metrics are presented in Table 3.

The contrast of the actual and predicted outer temperatures, inner temperature and PCM transition melting of the configuration (2) is illustrated in Fig. 13. The statistical analysis indicated that the network topology 2–8–8–4–6 is appropriate for the model. The MSE and R values for the network's outer temperature prediction are 0.0134 and 0.9977, respectively. The MSE and R values for the network's inner temperature

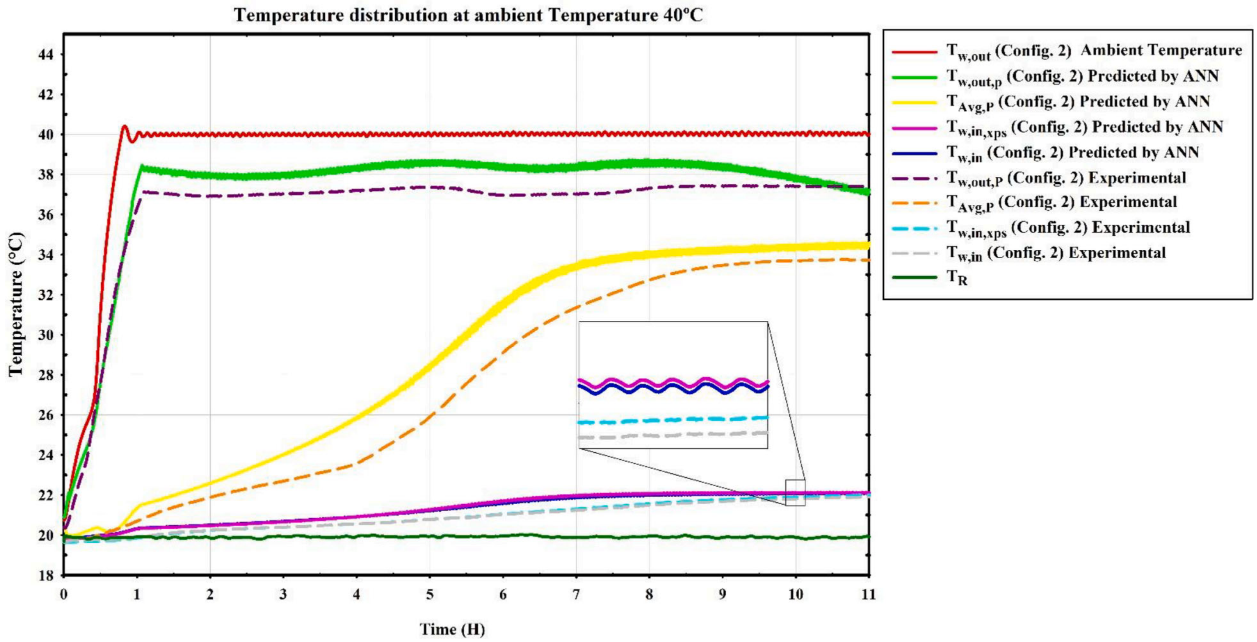

Fig. 14. Comparison between prediction and experimental for configuration (2) at 40 °C ambient temperature.

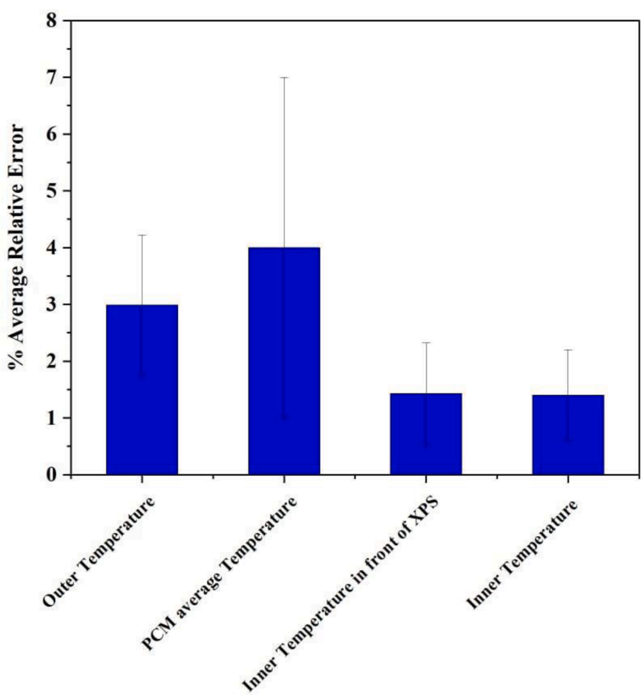

Fig. 15. Average relative error between Predicted by ANN and Experimental Testing.

prediction are 0.047 and 0.99542, respectively. At the same time, the MSE and R values for the network's PCM melting temperature prediction are 0.0234 and 0.9994, respectively. A strong correlation exists between the actual data derived from the experiment and the predicted data generated by the ANN model. Consequently, the ANN method serves as an efficient approach for studying the performance of PCM integrated into buildings and selecting a suitable location for PCM.

4.6. Prediction of temperature profiles of configuration (2) by ANN

To guarantee the accuracy and reliability of the prediction model utilizing the artificial neural network (ANN) in analyzing the performance efficiency of phase change materials in walls, the ANN was consulted to predict temperature patterns at an ambient temperature of 40 °C, even though 40 °C was not part of the training data. Fig. 14 shows a comparison of experimental testing and prediction models by ANN of the temperature profiles at different measurement points inside the experimental testing configuration (2), as depicted in Figure 5. The results show that the peak temperature of the external and inner walls in predictive simulation is 0.9 °C and 0.25 °C, respectively, greater than that observed in experimental testing. Additionally, the predictive simulation of PCM melting temperature is higher than experimental testing by 1.5 °C. It also demonstrates a strong correlation between experimental testing and predictive simulation. In addition to the qualitative evaluation of predicted, simulated, and experimental findings, the prediction model's accuracy is evaluated by relative errors. Fig. 15 shows that the average relative error in the data value is the discrepancy between the actual data and the predicted data for configuration (2) at an ambient temperature of 40 °C. The average relative error can be expressed according to Equation (5).

$$\textit{Relative Error}\ (\%) = \frac{\textit{True value} - \textit{Predicted value}}{\textit{True value}} \tag{5}$$

The figure shows the minimum and maximum relative errors for the indoor and outdoor temperatures in the ranges of (0.5–2 %) and (2–4 %), respectively. The relative error can be reduced by increasing experimental tests. This relative error range indicates a positive opinion about the use of artificial neural networks (ANNs) in the prediction performance of wall-integrated PCM.

4.7. Energy saving

Energy saving due to using PCMs integrated wall was calculated under various climatic conditions using equation (6) [43].

$$\textit{Energy saving}\ (ES) = \frac{Q_{ref} - Q_{PCM}}{Q_{ref}} \tag{6}$$

Where ES represents the energy saving ratio in %; and Q_{ref} and

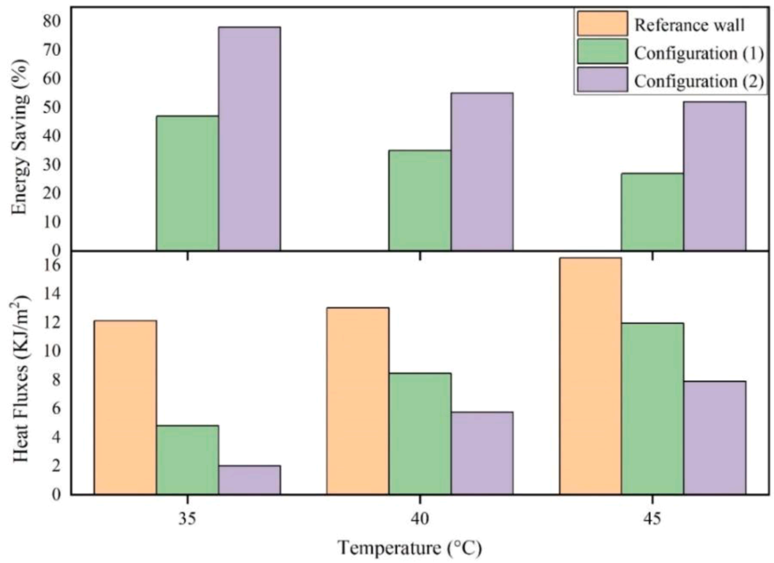

Fig. 16. Daily Heat Fluxes and Energy saving.

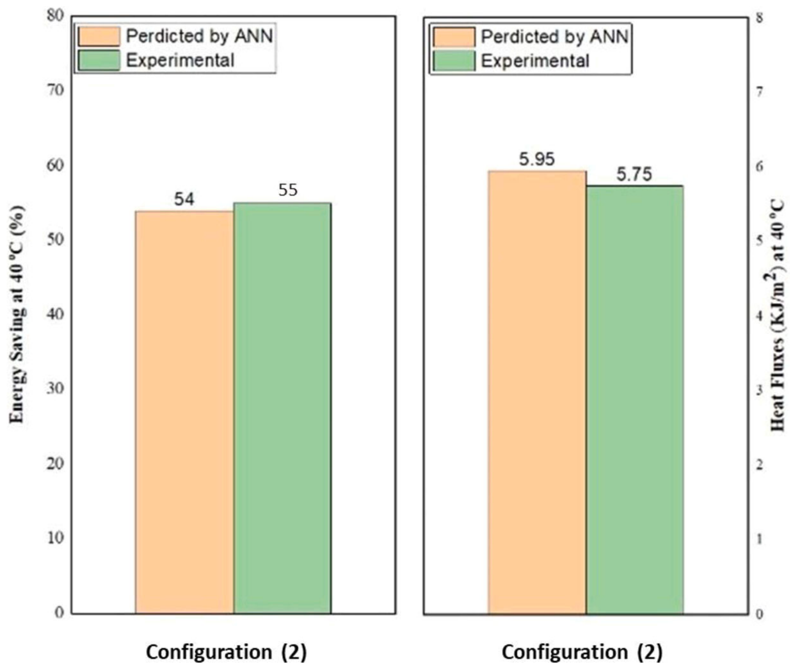

Fig. 17. Heat Fluxes and Energy saving for predicted by ANN and Experimental data.

Q_{PCM} denote the daily heat fluxes over the wall without and with the PCM cavity, measured in kJ/m^2, which are expressed as follows:

$$Q_{PCM} = \int_0^t q_{PCM}(t)dt \tag{7}$$

$$Q_{ref} = \int_0^t q_{ref}(t)dt \tag{8}$$

The daily performance for energy saving is analyzed while the PCM cavities are positioned adjacent to the outdoor surface as it is the case that gives better performance. Fig. 16 depicts the daily energy savings achieved by the utilization of phase change materials (PCMs) at different outside temperatures during the day for configurations (1) and (2) in comparison to the reference wall. Considering these circumstances, the peak heat fluxes in configuration (2) were evidently lower than those in configuration (1). As the outer surface temperature escalates, configuration (2) undergoes an augmentation in heat flux; however, it remains inferior to configuration (1). This resulted from the substantial latent heat absorption and storage capacity of the phase change materials (PCMs). The heat fluxes are substantial when the PCM cavities are placed adjacent to the external surface, in contrast to the heat fluxes on the outer surface. The daily heat fluxes were less when configuration (2) is positioned adjacent to the external surface, as the retained heat is dissipated more into the outer environment. The thermal resistance is greater, resulting in decreased performance when configuration (2) is implemented in a near-indoor environment. Energy savings from configuration (2) are evidently superior to those of configuration (1) across different ambient temperatures. The energy savings in configuration (1) are 47 %, 35 %, and 27 % for ambient temperatures of 35 °C, 40 °C, and 45 °C, respectively. The energy savings in configuration (2) for ambient temperatures of 35 °C, 40 °C, and 45 °C are 78 %, 55 %, and 52 %, respectively. The maximum heat fluxes on the internal surface were reduced for the walls with PCM cavities compared to the reference wall. The absorbed heat is retained within phase change materials, preventing its entry into the inside environment. The heat fluxes diminish when the PCM cavity is positioned adjacent to the interior surface. This occurred due to the reduced heat gain from the external surface. Fig. 17 illustrates a comparison between heat flux and energy saving predicted by ANN and experimental data for configuration (2) at an ambient temperature of 40 °C. The results show energy saving for both predicted data and experimental data is 54 % and 55 %, respectively. This result indicated that the prediction model can be utilized for the performance efficiency of PCM in the building.

5. Conclusions

Different configurations of PCMs integrated into prefabricated walls at different positions and thicknesses are experimentally investigated to determine the configuration of the best performance and energy savings. Furthermore, the artificial neural network is utilized to analyze the performance of configurations in terms of temperature profile and energy saving by training the artificial neural network at two ambient temperatures (35 °C and 45 °C) and then utilizing it to predict temperature profiles and energy saving at ambient temperature 40 °C. The following conclusions are derived from the results of this work.

- The use of PCM material in prefabricated walls reduces the external and internal surfaces temperatures of the wall, for example at the best PCM-wall configuration, the external and internal surfaces of the wall decrease by (3.1 °C, 2.7 °C, and 2. 3 °C) and (0.53 °C, 0.4 °C, and 0.25 °C), respectively at ambient temperature 35 °C,40 °C and 45 °C respectively.
- The PCMs discharge time decreases as the outdoor temperature increases, for example in configuration (2) the discharge times are 13 h, 10 h, and 8 h at ambient temperatures of 35 °C, 40 °C, and 45 °C, respectively. Average melting duration of PCM in configuration (2) is 3 h longer than in configuration (1) due to the increased PCM thickness.
- In Building cooling, the optimal location of the PCMs is to be near the outer wall surface as it lowers the wall peak temperature more than the case of locating PCM near the inner wall surface. The opposite is true in building heating where it is recommended to locate the PCM near the wall inner surface.
- The external and internal wall surfaces temperatures of configuration (2) were lower than the those of configuration (1) by 0.8575 °C and 0.4 °C, respectively at an ambient temperature 40 °C. The Internal surface temperature in configuration (2) is 0.4 °C lower than in configuration (1) at ambient temperature of 40C due to increased thermal resistance and reduced heat transmission.
- The peak heat fluxes in configuration (2) were evidently lower than those in configuration (1). due to the substantial latent heat absorption and retention. Nevertheless, the maximum heat fluxes on the internal surface were reduced for the walls containing PCM cavity.
- The energy saving in configuration (2) is higher than that in configuration (1), for example at an ambient temperature 40 °C the energy saving in Configurations 1 and 2 are 35 % and 55 %, respectively.
- The lower value of mean square error and high regression values for artificial neural network confirm the accuracy and reliability of the prediction model.
- This relative error range for predicted model at ambient temperature 40 °C indicates a good agreement to utilizing artificial neural network in the prediction performance of wall-integrated PCM without including ambient temperature in the training data set of artificial neural network.

Future research

Future research could explore the optimization of the configuration through the wall when integrated nanoparticles with PCM inside the configuration and validate the best configuration with ANN to predict the performance of configurations without training at a wide range of ambient temperatures and increase the input parameters, such as building material properties and other variables, to improve the accuracy of the prediction model.

CRediT authorship contribution statement

R.M. Saleh: Writing – original draft, Methodology, Investigation. **Mahmoud Said:** Writing – review & editing, Writing – original draft, Supervision. **W.G. Alshaer:** Writing – review & editing, Supervision. **S. A. Nada:** Writing – review & editing, Supervision.

Declaration of competing interest

The authors declare that they have no known competing financial interests or personal relationships that could have appeared to influence the work reported in this paper.

Data availability

Data will be made available on request.

References

[1] Z.A. Al-Absi, M.I.M. Hafizal, M. Asif, A. Alabdullatief, M. Ismail, Impacts of installation methods on the thermal performance of lightweight exterior cladding panels incorporating PCM: an experimental evaluation, Build Environ 265 (2024) 111964.

[2] J. Hou, Y. Huang, J. Zhang, X. Meng, B.J. Dewancker, Influence of phase change material (PCM) parameters on the thermal performance of lightweight building walls with different thermal resistances, Case Stud. Therm. Eng. 31 (2022) 101844.

[3] J. Hou, X. Meng, B.J. Dewancker, A numerical study on the effect of phase-change material (PCM) parameters on the thermal performance of lightweight building walls, Case Stud. Construct. Mater. 15 (2021) e00758.

[4] J. Hou, D. Wei, X. Meng, B.J. Dewancker, Thermal performance analysis of lightweight building walls in different directions integrated with phase change materials (PCM), Case Stud. Therm. Eng. 40 (2022) 102536.

[5] R.A. Kishore, C. Booten, M.V. Bianchi, J. Vidal, R. Jackson, Evaluating cascaded and tunable phase change materials for enhanced thermal energy storage utilization and effectiveness in building envelopes, Energy Build 260 (2022) 111937.

[6] W. Li, C. Feng, Y. Wang, J. Wang, X. Zhang, L. Zhang, Y. Dong, J. Zhao, Thermal performance analysis of lightweight phase change envelopes, Energy Build 323 (2024) 114850.

[7] M. Mahmoud, B.A. Yousef, A. Radwan, A. Alkhalidi, M.A. Abdelkareem, A. G. Olabi, Thermal assessment of lightweight building walls integrated with phase change material under various orientations, J. Build. Eng. 85 (2024) 108614.

[8] Z.-A. Liu, Y. Li, L. Tian, J. Hou, Q. Tang, W. Mo, X. Meng, Experimental analysis of the influence of PCM on the thermal behavior of lightweight buildings in different natural environments, Case Stud. Therm. Eng. 63 (2024) 105320.

[9] A.G. Anter, A.A. Sultan, A. Hegazi, M. El Bouz, Thermal performance and energy saving using phase change materials (PCM) integrated in building walls, J. Energy Storage 67 (2023) 107568.

[10] A.M. Nair, C. Wilson, M.J. Huang, P. Griffiths, N. Hewitt, Phase change materials in building integrated space heating and domestic hot water applications: a review, J. Energy Storage 54 (2022) 105227.

[11] R. Bruno, P. Bevilacqua, Bio-PCM to enhance dynamic thermal properties of dry-assembled wooden walls: experimental results, Build Environ 242 (2023) 110526.

[12] F. Ascione, N. Bianco, R.F. De Masi, M. Mastellone, G.P. Vanoli, Phase change materials for reducing cooling energy demand and improving indoor comfort: a step-by-step retrofit of a Mediterranean educational building, Energies. (Basel) 12 (19) (2019) 3661.

[13] A.A. Al-Rashed, A.A. Alnaqi, J. Alsarraf, Usefulness of loading PCM into envelopes in arid climate based on Köppen–Geiger classification-annual assessment of energy saving and GHG emission reduction, J. Energy Storage 43 (2021) 103152.

[14] K.O. Lee, M.A. Medina, E. Raith, X. Sun, Assessing the integration of a thin phase change material (PCM) layer in a residential building wall for heat transfer reduction and management, Appl Energy 137 (2015) 699–706.

[15] Z.A. Al-Absi, M.I.M. Hafizal, M. Ismail, A. Ghazali, Towards Sustainable development: Building's retrofitting With PCMs to Enhance the Indoor Thermal Comfort in Tropical Climate, Malaysia, Sustainability, 13 (7) (2021) 3614.
[16] Z.A. Al-Absi, M.H. Mohd Isa, M. Ismail, Phase change materials (PCMs) and their optimum position in building walls, Sustainability. 12 (4)) (2020) 1294.
[17] X. Jin, M.A. Medina, X. Zhang, Numerical analysis for the optimal location of a thin PCM layer in frame walls, Appl Therm Eng 103 (2016) 1057–1063.
[18] X. Jin, D. Shi, M.A. Medina, X. Shi, X. Zhou, X. Zhang, Optimal location of PCM layer in building walls under Nanjing (China) weather conditions, J Therm Anal Calorim 129 (2017) 1767–1778.
[19] A. Refahi, A. Rostami, M. Amani, Implementation of a double layer of PCM integrated into the building exterior walls for reducing annual energy consumption: effect of PCM wallboards position, J. Energy Storage 82 (2024) 110556.
[20] X. Sun, J. Jovanovic, Y. Zhang, S. Fan, Y. Chu, Y. Mo, S. Liao, Use of encapsulated phase change materials in lightweight building walls for annual thermal regulation, Energy 180 (2019) 858–872.
[21] R.J. Khan, M.Z.H. Bhuiyan, D.H. Ahmed, Investigation of heat transfer of a building wall in the presence of phase change material (PCM), Energy Built Environ. 1 (2) (2020) 199–206.
[22] V.D. Cao, T.Q. Bui, A.-L. Kjøniksen, Thermal analysis of multi-layer walls containing geopolymer concrete and phase change materials for building applications, Energy 186 (2019) 115792.
[23] M. Arıcı, F. Bilgin, S. Nižetić, H. Karabay, PCM integrated to external building walls: an optimization study on maximum activation of latent heat, Appl Therm Eng 165 (2020) 114560.
[24] A. Lagou, A. Kylili, J. Šadauskienė, P.A. Fokaides, Numerical investigation of phase change materials (PCM) optimal melting properties and position in building elements under diverse conditions, Constr. Build. Mater. 225 (2019) 452–464.
[25] F. Darvishi, E. Markarian, N. Ziasistani, N. Ziasistani, A. Javanshir, Energy performance assessment of PCM buildings considering multiple factors, in: 2019 International Conference on Power Generation Systems and Renewable Energy Technologies (PGSRET), IEEE, 2019, pp. 1–5.
[26] R.A. Kishore, M.V. Bianchi, C. Booten, J. Vidal, R. Jackson, Parametric and sensitivity analysis of a PCM-integrated wall for optimal thermal load modulation in lightweight buildings, Appl Therm Eng 187 (2021) 116568.
[27] R. Olu-Ajayi, H. Alaka, H. Owolabi, L. Akanbi, S. Ganiyu, Data-driven tools for building energy consumption prediction: a review, Energies. (Basel) 16 (6) (2023) 2574.
[28] Z. Chen, F. Xiao, F. Guo, J. Yan, Interpretable machine learning for building energy management: a state-of-the-art review, Adv. Appl. Energy 9 (2023) 100123.
[29] A. Fallahpour, K.Y. Wong, S. Rajoo, G. Tian, An evolutionary-based predictive soft computing model for the prediction of electricity consumption using multi expression programming, J Clean Prod 283 (2021) 125287.
[30] R. Olu-Ajayi, H. Alaka, I. Sulaimon, F. Sunmola, S. Ajayi, Machine learning for energy performance prediction at the design stage of buildings, Energy Sustain. Develop. 66 (2022) 12–25.
[31] M. Lin, L. Peng, T. Liu, L. Zhang, Novel approach to energy consumption estimation in smart homes: application of data mining and optimization techniques, Front. Energy Res. 12 (2024) 1361803.
[32] F. Jiang, J. Ma, Z. Li, Y. Ding, Prediction of energy use intensity of urban buildings using the semi-supervised deep learning model, Energy 249 (2022) 123631.
[33] L.T. Le, H. Nguyen, J. Dou, J. Zhou, A comparative study of PSO-ANN, GA-ANN, ICA-ANN, and ABC-ANN in estimating the heating load of buildings' energy efficiency for smart city planning, Appl. Sci. 9 (13) (2019) 2630.
[34] K. Nazir, S.A. Memon, A. Saurbayeva, A. Ahmad, Energy consumption predictions by genetic programming methods for PCM integrated building in the tropical savanna climate zone, J. Build. Eng. 68 (2023) 106115.
[35] H. Yang, Z. Xu, Y. Shi, W. Tang, C. Liu, A. Yunusa-Kaltungo, H. Cui, Multi-objective optimization designs of phase change material-enhanced building using the integration of the stacking model and NSGA-III algorithm, J. Energy Storage 68 (2023) 107807.
[36] H. Bagheri-Esfeh, H. Safikhani, S. Motahar, Multi-objective optimization of cooling and heating loads in residential buildings integrated with phase change materials using the artificial neural network and genetic algorithm, J. Energy Storage 32 (2020) 101772.
[37] M. Zhussupbekov, S.A. Memon, S.A. Khawaja, K. Nazir, J. Kim, Forecasting energy demand of PCM integrated residential buildings: a machine learning approach, J. Build. Eng. 70 (2023) 106335.
[38] RUBITHERM-RT®, phase change material 2024,technical datasheets of RT24, (accessed on 5 April 2024).
[39] M. Nazari Sam, A. Caggiano, C. Mankel, E. Koenders, A comparative study on the thermal energy storage performance of bio-based and paraffin-based PCMs using DSC procedures, Materials (Basel) 13 (7) (2020) 1705.
[40] R.J. Moffat, Describing the uncertainties in experimental results, Exp. Therm. Fluid. Sci. 1 (1) (1988) 3–17.
[41] C. Zhang, Y. Chen, L. Wu, M. Shi, Thermal response of brick wall filled with phase change materials (PCM) under fluctuating outdoor temperatures, Energy Build 43 (12) (2011) 3514–3520.
[42] M. Alibeigi, R. Jazmi, R. Maddahian, H. Khaleghi, Integrated study of prediction and optimization performance of PBI-HTPEM fuel cell using deep learning, machine learning and statistical correlation, Renew Energy 235 (2024) 121295.
[43] Q. Wang, R. Wu, Y. Wu, C. Zhao, Parametric analysis of using PCM walls for heating loads reduction, Energy Build 172 (2018) 328–336.